LAWRENCE
LIVERMORE
NATIONAL
LABORATORY

LLNL-CONF-656294

Microwave Interferometry for Understanding Deflagration-to-Detonation and Shock-to-Detonation Transitions in Porous Explosives

J. W. Tringe, R. J. Kane, K. S. Vanderall, M. C. Converse, F. Garcia, C. M. Tarver

June 30, 2014

15th International Detonation Symposium
San Francisco, CA, United States
July 13, 2014 through July 18, 2014

Disclaimer

Microwave Interferometry for Understanding Deflagration-to-Detonation and Shock-to-Detonation Transitions in Porous Explosives

Joseph W. Tringe, Ron J. Kane, Kevin S. Vandersall,
Mark C. Converse, Frank Garcia and Craig M. Tarver

Energetic Materials Center
Lawrence Livermore National Laboratory, Livermore, CA 94550

Abstract. Diagnostics to interrogate shock and deflagration fronts *in situ* without embedded sensors are desirable to improve the understanding of front initiation and propagation. Here we report on microwave interferometry (MI)[1-5] measurements that have been successfully used for characterization of deflagration-to-detonation transition (DDT) and shock-to-detonation transition (SDT) events in porous energetic materials. We use frequencies in the range 12.5-26.6 GHz to observe the development of detonation fronts which are highly reflective to microwaves. In this work, the MI technique was used to measure the transition to detonation in both DDT and SDT scenarios for porous explosives HMX and Composition B. Data was obtained through a silica window for the case of DDT and inside a non-ideal waveguide in an SDT configuration using appropriate coupled waveguides. The calculated velocities based on the MI Doppler period were comparable but higher than were measured with ionization pins (DDT) and Manganin gauges (SDT), with better agreement to the Manganin gauge data in the SDT experiment. Details of the approach and measurements are presented together with a discussion of the possible use of this technique to measure the in situ fraction reacted, with insights on frequency ranges and configurations desired to make this an effective measurement.

Introduction

Microwave interferometry (MI) is well-suited to characterize reacting fronts in explosives since microwaves can penetrate deep into explosive samples without modifying the material and provide information on the position of fronts with ~mm scale spatial resolution.[1, 2, 4, 6-8] A second advantage of MI is that the amplitude of the return signal may be correlated with the density of hot spots being created by a developing detonation wave.[8] However, phenomena such as deflagration-to detonation transition (DDT) often require heavy confinement by metal cases which present an obstacle to microwave interrogation. Other gun-type shock-to-detonation (SDT) experiments can present a large-area detonating surface inside an insulating cylinder to a smaller microwave probe such that the microwaves do not propagate through an ideal waveguide. In this work we demonstrate experimental conditions which enable characterization of heavily-confined and large-area, insulator-confined detonating surfaces with MI. We also apply the Ignition and Growth model to porous explosives, and compare the predictions of this model with our observed MI data to provide insight into the mechanisms underlying transitions to detonation.

Experimental configuration

For the characterization of DDT, 12.5 GHz signals launched at 13 dBm were reflected from a detonation front developed in a cylinder of HMX powder. The powder was heavily confined in a steel cylinder with a 25.4 mm inner diameter, 76.2 mm outer diameter and an overall length of 342.8 mm; it was hand packed to ~62% theoretical maximum density (TMD). Microwave signals were launched from a waveguide proximate to a conical silica window, 25.4 mm high, located at the end of the cylinder remote from the DDT initiation location. Ignition was initiated with a thermite ignitor as described previously.[4, 9] MI results were correlated with times from 15 ionization pins inserted through the exterior metal wall along the length of the cylinder. Figure 1 shows the geometry as simulated using the Ansys HFSS (High Frequency Structural Simulator) finite element code with an inset displaying a photograph of the silica window configuration used for this experiment.

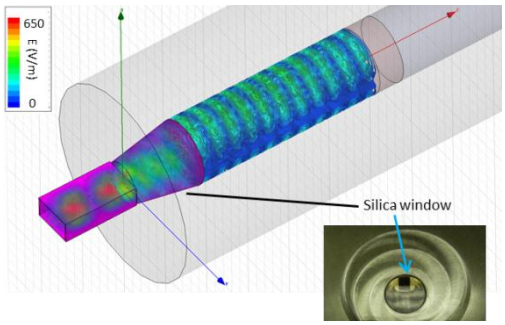

Figure 1. HFSS Simulation of DDT geometry. False color indicates magnitude of the electric field. Inset: photo of the remote end of the conical silica window through which microwave signals are introduced into the explosive cylinder.

MI was also used to characterize the shock-to-detonation transition (SDT) in a porous bed of Composition B hand packed to ~64% TMD as shown in Figure 3. Manganin piezoresistive pressure gauges were placed between each explosive layer. Explosive layers were packed inside Teflon rings with an inner diameter of 70 mm, outer diameter of 90 mm, and thicknesses varying from 3 to 10 mm. A sabot with a Teflon flyer was used to impact a 5 mm thick aluminum plate in front of the explosive at 540 m/s. The impact event was interrogated with a 0 dBm 26.6 GHz signal launched from a waveguide behind the explosive and a 10 mm thick Teflon backing plate.

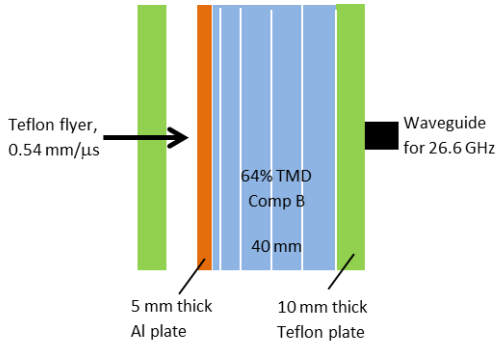

Figure 2. Experimental geometry of porous Comp B impacted by a Teflon flyer. Manganin gauges are placed between porous layers at 0, 3, 10, 20, 30 and 40 mm depth relative to the Al plate interface.

Experimental Results

After analysis of the microwave signals for the DDT experiment, the expected interference-generated sinusoidal pattern is observed soon after the acceleration of the deflagration front into a detonation front. This data, shown in Figure 2 superimposed with the pin timing, is obtained by multiplying the carrier signal with the reflected wave signal, followed by low-pass filtering of the product. The reflected power as a function of detonation front position was predicted by the HFSS simulation and correlates well with this signal history assuming the detonation front is an ideal reflecting surface.

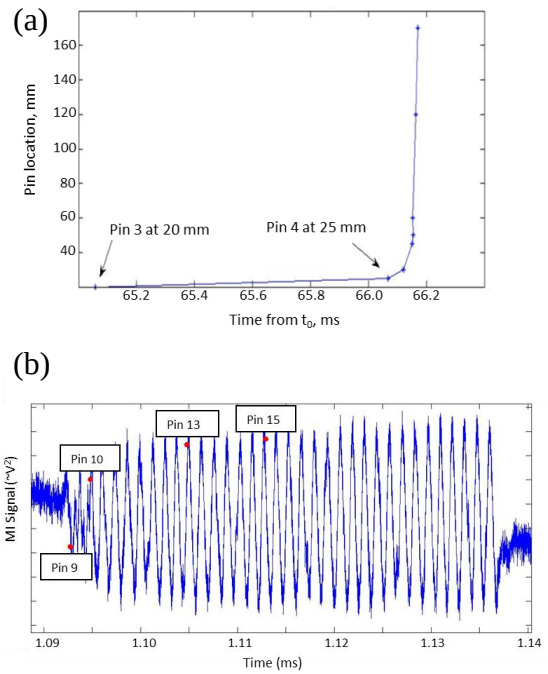

Figure 3. (a) Pin time as a function of position within the HE column (b) Sinusoidal pattern of reflected microwave energy, with pin timing indicators superimposed

From Figure 3(a), key pin positions and times are summarized in Table 1.

Table 1. Time, position, 2-point velocity for pins

Pin #	Time ms	Position mm	Velocity mm/μs
3	65.058	20	-
4	66.067	25	0.56
5	66.120	30	0.09
8	66.151	45	0.48
10	66.153	60	7.50
13	66.163	120	6.00
15	66.171	170	6.25

For the SDT experiment, data from a subset of the Manganin gauge records is shown in Figure 4. The low pressure at the gauge at 3 mm suggests that detonation has not yet initiated in this position. A much more abrupt pressure rise is observed at the gauge at 10 mm, however. The amplitude of the pressure rise approximately doubles by the time the pulse reaches the gauge at 20 mm, approximately 3 μs later, indicating that a well-defined detonation wave has formed.

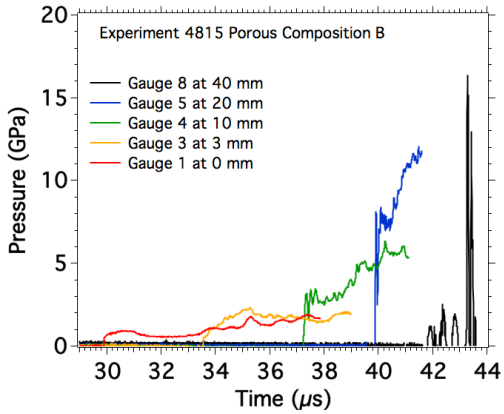

Figure 4. Pressure as a function of time from five Manganin gauges distributed at 0, 3, 10, 20 and 40 mm into the Comp B explosive.

Figure 5 shows the gauge arrival timing as a function of position for the 6 Manganin gauges. Here time is taken to be relative to the first gauge's reporting time. This data indicates that a detonation wave likely forms between 7 and 10 microseconds after the explosive impact, and that the velocity of the detonation wave is 5.94 mm/μs.

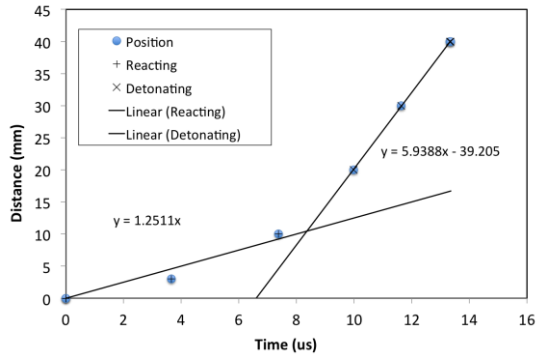

Figure 5. Manganin gauge position vs. reporting time. Detonation appears to initiate between 7 and 10 μs after the reporting of the first gauge at time 0 with a detonation velocity of 5.94 mm/μs.

MI data for the full shot record is shown in Figure 6(a). As was done for the DDT experiment, this data was obtained by multiplying the carrier signal with the reflected wave signal, then low-pass filtering the product. A moving detonation wave or other reflected front is expected to produce an oscillating signal because of the time-varying change of phase of the reflected signal. The time period of the shock transit and initiation is shown highlighted in a box in Figure 6(a).

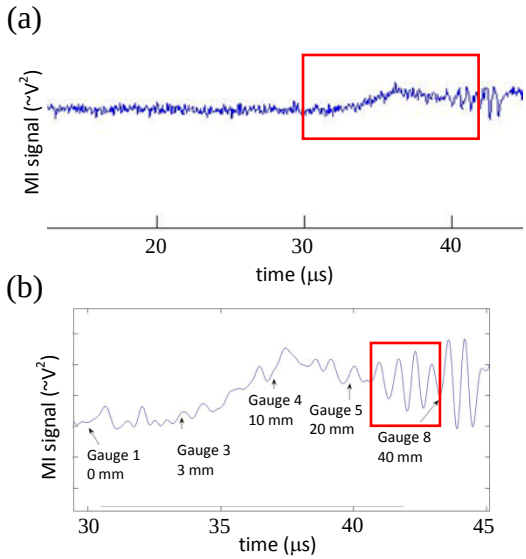

Figure 6. (a) MI for the full shot record time with 0 time referenced to the same value used for the Manganin gauge data shown in Figure 2. The times shown in (b) are highlighted by a box. (b) Expanded view of MI record, with best-defined oscillating signal highlighted by a box. Additional periods beyond gauge 8 are not included because these correspond to time after the detonation wave transits the explosive/Teflon interface.

An expanded view of Figure 6(a) is shown in Figure 6(b) with Manganin gauge timing indicated by arrows. A steady rise in amplitude begins soon after the reporting time for Gauge 3, 3 mm into the Comp B. Although the arrival time of the detonation wave at Gauge 8 at the end of the 40 mm of Comp B is not particularly well-defined, it appears that the oscillating MI record may persist after the arrival of the detonation wave at the Teflon at ~43 μs. There may also be a time offset related to a curved detonation front and the fact that the microwave waveguide was radially offset from center.

Ignition and Growth Modeling of Low Density Composition B Shock Initiation

The Ignition and Growth reactive flow model [10-12] uses two Jones-Wilkins-Lee (JWL) equations of state (EOS) in the temperature dependent form:

$$p = Ae^{-R_1 V} + Be^{-R_2 V} + \omega C_v T/V \qquad (1)$$

where p is pressure, V is relative volume, T is temperature, ω is the Gruneisen coefficient, C_v is the average heat capacity, and A, B, R_1 and R_2 are constants. The reaction rate equation is:

$$dF/dt = \underbrace{I(1-F)^b(\rho/\rho_0 - 1 - a)^x}_{0<F<F_{Ig\,max}} + \underbrace{G_1(1-F)^c F^d p^y}_{0<F<F_{G_1\,max}} + \underbrace{G_2(1-F)^e F^g p^z}_{F_{G_2\,min}<F<1} \qquad (2)$$

where F is fraction reacted, t is time in μs, ρ is current density, ρ_o is initial density, p is pressure in Mbars, and I, G_1, G_2, a, b, c, d, e, g, x, y, and z are constants. A set of parameters for Composition B at high density (1.712 g/cm^3) were developed by Urtiew et al.[13] based on embedded mangnain pressure gauge records and other shock initiation data. To model lower density shock initiation, the unreacted JWL EOS was modified based on the lower strength and sound velocity of the porous explosive by lowering the value of A for the unreacted Composition B, and the fraction ignited F_{igmax} parameter was increased from 0.022 to 0.09 to account for the greater number of hot spot formation sites. A new JWL product equation for Composition B based on detonation and overdriven experimental data[14] was also used in this modeling. Similar changes were also made for modeling the shock initiation of two lower initial densities of HMX, including the 1.2 g/cm^3 material used in the DDT experiments.[15, 16] Table 2 lists the parameters for the 1.115 g/cm^3 Composition B in this shock initiation shot.

Table 2. Composition B modeling parameters

Initial density ρ_O =1.115 g/cm^3		
Unreacted JWL	Product JWL	Reaction Rates
A = 100.0 Mbar	A = 13.4815 Mbar	I = 4.0x10^6 μs^{-1} F_{igmax}= 0.09
B=-0.024337 Mbar	B = 0.5896 Mbar	a = 0.0367 b = 0.667
R_1 = 11.3	R_1 = 6.2	x = 7.0
R_2 = 1.13	R_2 = 2.2	G_1 = 140 Mbar$^{-2}\mu s^{-1}$ F_{G1max} = 0.7
ω = 0.8938	ω = 0.5	c = 0.667 d = 0.333
Cv = 2.487x10^{-5} Mbar/K	Cv = 1.0x10^{-5} Mbar/K	y = 2.0
To = 298°K	Eo = 0.0544 Mbar	G_2 = 1000 Mbar$^{-3}\mu s^{-1}$ F_{G2min} = 0
Shear Mod = 0.017 Mbar		e = 0.222 g = 1.000
Yield Str = 0.002 Mbar		z = 3.0

The results of modeling the SDT experiment are shown in Figs. 7 and 8. Figure 7 shows the calculated pressure histories for the six Manganin gauges, and Fig. 8 shows the corresponding fraction reacted histories in the Composition B next to the gauges. The calculated pressure increases in Fig. 7 are similar to the measured pressures in Fig. 4. The increases in fractions reacted as functions of time and distances in Fig. 8 are the direct causes of the MI signals.

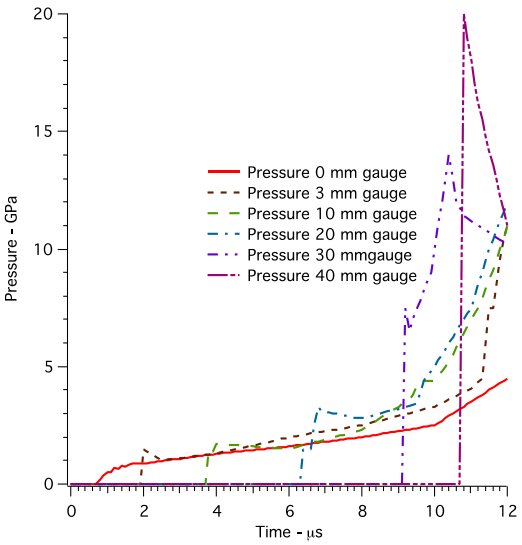

Figure 7. Calculated pressure histories in reacting Composition B during the SDT experiment with Manganin data shown in Figures 4 and 5.

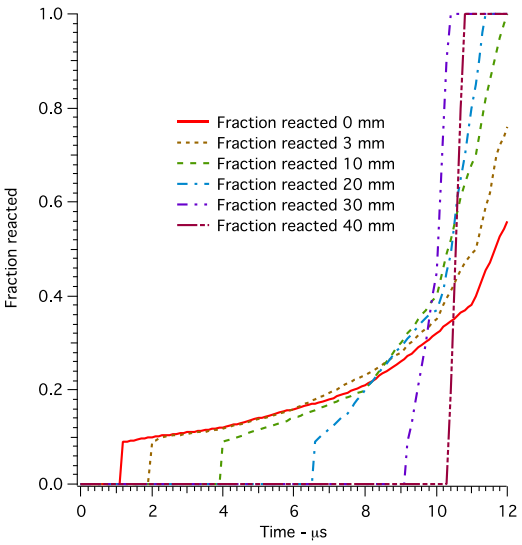

Figure 8. Calculated fraction reacted histories in Composition B during the SDT experiment with Manganin data shown in Figures 4 and 5.

Discussion

Hot spot formation is critical for both DDT and SDT processes. During DDT, there is a progression of reactive flow processes that occur: conductive deflagration, convective deflagration,

coalescence of pressure wavelets to form a solid plug behind a leading shock wave, and finally SDT in the porous explosive beyond the plug. The density and size of hot spots rapidly accelerates during these events. A complex model of these deflagration and porous compaction processes has been developed in ALE3D by Kercher et al.[15] For the SDT process, Kercher et al. used the Ignition and Growth model that has recently been parameterized for low-density HMX (65% TMD) using embedded Manganin pressure gauge data.[16]

In general the velocity of the detonation wave may be independently estimated from the period of the MI signal oscillation. The front velocity U_s is calculated from the Doppler period T of the return signal and the microwave wavelength, λ_g, inside the interrogated medium:

$$U_s = \frac{\lambda_g}{2T} \qquad (3)$$

λ_g can be estimated by:

$$\lambda_g = \frac{\lambda_0}{\lambda_0\sqrt{\epsilon_r - \left(\lambda_0/\lambda_c\right)^2}} \qquad (4)$$

where λ_0 is the vacuum wavelength of the microwave signal. λ_c is the cutoff wavelength of the signal in the waveguide. ϵ_r is the relative dielectric constant of the medium at the interrogation frequency.[8] For a circular waveguide with radius r, the cutoff wavelength for the dominant TE_{11} mode is in vacuum given by:

$$\lambda_{c,0} = \frac{2\pi r}{1.8412} \qquad (5)$$

Since the waveguide is filled with a dielectric with ϵ_r, $\lambda_c = \lambda_{c,0}/\sqrt{\epsilon_r}$. We estimate the dielectric constant of the porous explosive, ϵ_{powder}, using the unified mixing equation:

$$\frac{\epsilon_{powder}-1}{\epsilon_{powder}-2+\nu(\epsilon_{powder}-1)} = f\frac{\epsilon_{exp}-1}{\epsilon_{exp}-2+\nu(\epsilon_{exp}-1)} \qquad (6)$$

where f is the fraction of explosive in the explosive powder/air mixture, ϵ_{exp} is the dielectric constant of explosive at 100% TMD, and ν is a dimensionless parameter that depends on the solid permittivity and its volume fraction.[17, 18]

For the HMX DDT experiment we assume the dielectric constant of HMX, ϵ_{HMX}, at the measurement frequency 12.5 GHz (λ_0 = 23 mm) has the same value as has been estimated at 10 GHz, 3.48.[19] We further assume that the volume fraction f is 0.62, and ν from Equation 4 for this dielectric constant and volume fraction is 1.2.[18] The Doppler period T is 1.3 μs (Figure 3(b)). Using Equations 1-4 with these values leads to a ~30% overestimate of the 6.1 mm/μs ionization pin-measured detonation velocity. This difference is not likely due to compaction of the HMX powder ahead of the detonation wave. From Equations 3-6, we estimate that the HMX powder would need to be almost ~90% TMD to create the $\epsilon_r = \epsilon_{powder} = 2.84$ which would be necessary to account for the apparently increased velocity as determined by MI. Additional experiments are necessary to demonstrate the lack of compaction, however.

For the Comp B SDT experiment the beginning of the best-defined oscillations at ~37 μs in principle corresponds to the initiation of the detonation wave. Since the gauge at 0 mm reports at 30 μs, this time corresponds to ~7 μs after the gauge reports, consistent with the times reported by subsequent Manganin gauges as shown in Figures 4 and 5.

We assume that ϵ_{CompB} at 26.6 GHz (λ_0 = 11 mm) has the same value as has been estimated at 10 GHz, 3.29.[19] The value of f is known from the density of the pellets to be 0.64, and ν for this dielectric constant and volume fraction is also 1.2.[18] We also assume the waveguide has the radius of the Comp B cylinders, 70 mm, so that $\lambda_c = \lambda_{c,0}/\sqrt{\epsilon_r}$ = 8.64 cm with $\epsilon_r = \epsilon_{powder}$ = 1.91 from Equation 4. From the data shown in Figure 6(b), there are at least three unambiguous cycles in the MI signal over 1.9 μs immediately before the last Manganin gauge report time, so that T = 0.64 μs. Then from the above parameters and Equations 3 and 4, the calculated U_s = 6.5 mm/μs. This represents a ~10% overestimate relative to the 5.9 mm/μs determined by the Manganin gauges.

Interestingly, we observe there is slower increase in MI signal amplitude starting about a microsecond before Manganin gauge 3 reports at 3 mm beyond the aluminum barrier. The amplitude peaks about 0.7 μs later. If we take this time to be half a Doppler period, then the implied velocity is 420 m/s, which is comparable 540 m/s impact velocity of the Teflon flyer into the aluminum barrier in front of the Comp B.

As previously noted, microwave reflections resolve to an unambiguous high-frequency Doppler period (Figure 6) at about 2 microseconds before the Manganin gauge at 40 mm reports. This gauge shows a fast pressure rise which we attribute to a detonation wave. From the fraction reacted history calculated with the Ignition and Growth model shown in Figure 8, the 2 microseconds preceding the 40 mm gauge corresponds to about 20% reacted throughout the depth of the explosive. The amplitude increase of the MI signal over this time period then corresponds to the faster reaction of the explosive in the 20-40 mm depth of the explosive. Unfortunately more quantitative analysis is complicated by the small number of Doppler periods over the transition time in this experiment, and the fact that the transition to detonation corresponds with the end of the explosive sample so that a steady-state condition is not observed. In the future with higher frequency interrogation, however, MI may be used more effectively to calibrate the Ignition and Growth model by more accurately and directly measuring the reacted fraction.

Conclusions

We experimentally demonstrate that MI can be employed to measure the transition to detonation in both DDT and SDT scenarios for porous explosives HMX and Composition B. Useful data is obtained through a silica window (DDT) and inside a non-ideal waveguide (SDT) using appropriate coupled waveguides. The calculated velocities based on the MI Doppler period are comparable but higher than were measured with ionization pins and Manganin piezoresistive gauges, with better agreement to the Manganin gauge data in the SDT experiment. We also present results of calculations made with the Ignition and Growth model for low-density HMX powder and Composition B. For Composition B impacted by a 540 m/s Teflon flyer, the calculated transition to detonation time and pressures matches the transition characterized by the Manganin gauge record. Additional information about the fraction reacted in the Ignition and Growth model may be provided by MI data, but higher frequency interrogation or a longer transition to steady state are needed to more conclusively demonstrate this correlation.

Acknowledgements

This research was partially supported by the Joint DoD-DOE Munitions Technology Development Program. This work performed under the auspices of the U. S. Department of Energy by Lawrence Livermore National Laboratory under Contract DE-AC52-07NA27344.

References

1. V. M. Bel'skii, A. L. Mikhailov, A. V. Rodionov and A. A. Sedov, Combustion Explosion and Shock Waves **47** (6), 639-650 (2011).
2. G. F. Cawsey, J. L. Farrands and S. Thomas, Proceedings of the Royal Society of London Series a-Mathematical and Physical Sciences **248** (1255), 499-521 (1958).
3. M. A. Cook, R. L. Doran and G. J. Morris, Journal of Applied Physics **26** (4), 426-428 (1955).
4. B. C. Glancy, A. D. Krall and H. W. Sandusky, Shock Waves in Condensed Matter 1987. Proceedings of the American Physical Society Topical Conference, 711-714 (1988).
5. P. J. Rae, B. B. Glover, J. A. Gunderson and W. L. Perry, in *Shock Compression of Condensed Matter - 2011, Pts 1 and 2*, edited by M. L. Elert, W. T. Buttler, J. P. Borg, J. L. Jordan and T. J. Vogler (2012), Vol. 1426.
6. J. L. Farrands and G. F. Cawsey, Nature **177** (4497), 34-35 (1956).
7. B. C. Glancy, H. W. Sandusky and A. D. Krall, Journal of Applied Physics **74** (10), 6328-6334 (1993).

8. A. D. Krall, B. C. Glancy and H. W. Sandusky, Journal of Applied Physics **74** (10), 6322-6327 (1993).
9. H. W. Sandusky and R. H. Granholm, in *Shock Compression of Condensed Matter - 2007, Pts 1 and 2*, edited by M. Elert, M. D. Furnish, R. Chau, N. C. Holmes and J. Nguyen (2007), Vol. 955, pp. 991-996.
10. E. L. Lee and C. M. Tarver, Physics of Fluids **23** (12), 2362-2372 (1980).
11. C. M. Tarver, J. W. Kury and R. D. Breithaupt, Journal of Applied Physics **82** (8), 3771-3782 (1997).
12. C. M. Tarver, Propellants Explosives Pyrotechnics **30** (2), 109-117 (2005).
13. P. A. Urtiew, K. S. Vandersall, C. M. Tarver, F. Garcia and J. W. Forbes, Russian Journal of Physical Chemistry B **2** (2), 162-171 (2008).
14. C. M. May and C. M. Tarver, Journal of Physics: Conference Series **500**, 052045 (2014).
15. J. R. Kercher, C. M. Tarver, V. P. Georgevich, J. L. Maienschein, D. E. Stevens, W. B. Bateson, P. Pincosy, T. Dunn, H. K. Springer and A. Nichols, (unpublished, 2013).
16. F. Garcia, K. S. Vandersall and C. M. Tarver, Journal of Physics: Conference Series **500**, 052048 (2014).
17. A. H. Shivola, IEEE Transactions on Geoscience and Remote Sensing **27** (4), 403-415 (1989).
18. B. B. Glover and W. L. Perry, Propellants Explosives Pyrotechnics **34** (4), 347-350 (2009).
19. M. Daily, B. Glover, S. Son and L. Groven, Propellants Explosives Pyrotechnics **38** (6), 810-817 (2013).

Question

James Ferguson, AWE
Is there a spot size associated with the measurement or is it an average across the wave front?

Reply by Joe Tringe and Ron Kane
In general, the measurement is an average across the front, and is sensitive to the component of the front velocity which is parallel to the interrogating microwave beam path.

Question

David Kittell, Purdue University
In the raw interferometer signal for steady detonation, there is amplitude variation. We think this to be due to the number of pressed increments. How did you press and prepare your samples?

Reply by Joe Tringe and Kevin Vandersall
The DDT samples were lightly hand pressed incrementally, such that small-scale density variations on the order of a few percent are possible with a spatial period of about an inch. In the Composition B experiment, the powder Composition B was lightly hand tamped within each ring before adding on additional layers. Small density variations between each layer for this geometry are also expected on the order of each layer thickness.

Question

Jake Gunderson, LANL
How were the Manganin gauges arranged to allow simultaneous RF measurements?

Reply by Joe Tringe and Ron Kane
Manganin gauges (~10 mm wide foil) were rotated such that a clear line of sight existed through the explosive from the microwave wave guide (placed off axis from the centerline) to the impacted aluminum metal surface. As part of the assembly, the Teflon gauge package that armors each gauge was still present between each Composition B layer in the line of sight of the microwaves.